Surface diffusion and growth of patterned nanostructures on strained surfaces

R. F. Sabiryanov,[1] M. I. Larsson,[1,*] K. J. Cho,[2] W. D. Nix,[1] and B. M. Clemens[1]
[1]*Department of Materials Science and Engineering, Stanford University, Stanford, California 064312*
[2]*Department of Mechanical Engineering, Stanford University, Stanford, California 064312*
(Received 26 August 2002; revised manuscript received 25 November 2002; published 18 March 2003)

We propose a method of controllable growth of patterned nanostructures on a surface with a self-organized network of buried dislocations. The general treatment for the diffusion of Co adatoms and growth on the strained Pt surface is given as a prototype for magnetic recording media. *Ab initio* self-consistent calculations of surface diffusion events of a Co adatom on the Pt(111) surface show that adatoms prefer to diffuse to the regions of largest tensile strain. The hopping barrier for adatom diffusion increases with tensile strain showing that preferred nucleation occurs in the regions of high tensile stress. The variation of the hopping barrier on the underlying strain produced by buried dislocations is analyzed in terms of a surface stress relief picture based on *ab initio* calculations. Based on these results, kinetic Monte Carlo studies of the growth of Co on Pt(111) have been performed; they show the possibility of controlled growth of patterned nanostructures with appropriate choice of dislocation spacing, film thickness and temperature.

DOI: 10.1103/PhysRevB.67.125412 PACS number(s): 68.35.Ja

I. INTRODUCTION

Computational nanoengineering is an emerging field of materials research, leading to nanoscale modeling and simulation methods which enable and accelerate the design and development of functional nanometer-scale devices and systems. Just as microfabrication has led to the microelectronics revolution in the 20th century, nanoprecision engineering will be a key to the nanotechnology revolution in the 21st century. A major challenge in this technology is to fabricate patterned nanostructures.

The growth of magnetic metal films on metal substrates is a long-standing problem and has been actively studied for many years and especially for magnetic recording.[1] One of the main interests has been to study the interplay between surface geometry and growth with the ultimate objective of fabricating of controlled nanoscale structures. Growth of patterned arrays of magnetic nanoparticles may allow further increases in recording density. The present study concentrates on Co growth on strained thin Pt films. This system has potential application as magnetic recording media because hcp Co as well as Co-Pt multilayers and alloys have strong uniaxial anisotropy.[2] The anisotropy direction and strength of Co-Pt is strongly affected by the geometry of the system, and practical use of this system requires controlled growth of Co on Pt.

Vertical pillars has been fabricated by self-assembly and self-organization on the reconstructed surfaces.[3] In the present paper we show that pillars can be fabricated using the concept of self-organization due to elastic strain on the surface. The attractive part of our approach is that the size and distance between pillars can be *controlled*.

The general idea is presented in Figs. 1(a) and 1(b). For example, a thin film of Pt can be deposited on the clean flat surface of sapphire. Due to the mismatch of the lattice constants, dislocations evolve in the Pt film when it is relaxed. These dislocations repel each other so that the equilibrium configuration is given by an equally spaced dislocation array. Such well-spaced arrays have been observed experimentally.[4] The buried dislocations produce a long-range elastic strain field. If the Pt film is thin enough, the field will give rise to a sizable periodic strain at the surface of the Pt film. At the initial stage of the deposition process, Co atoms adsorb on the Pt surface. The interactions between Co adatoms and Pt surface atoms, as well as interactions of Co atoms among themselves, determine the original nucleation sites. The adatoms, deposited on the periodically strained surface, will diffuse and nucleate according to the surface strain modulation.

The paper is organized in the following way. In Sec. II, we present density functional theory (DFT) calculations of the diffusion energy barrier of a Co adatom on Pt(111) surfaces in the presence of surface strain to determine the underlying mechanisms of the growth process. The first question we will study is the question of which are the preferred nucleation sites for Co. In Sec. III, the linear elastic theory is applied to explain the trends obtained in DFT simulations. Section IV presents simulation of the growth; the kinetic Monte Carlo (KMC) method[5] is used with the important rates calculated from first principles using DFT.

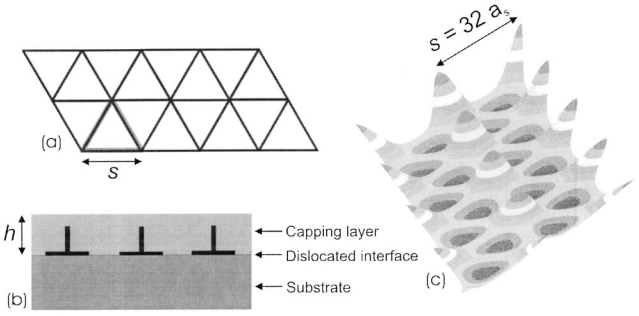

FIG. 1. (a) Top view of the hexagonal dislocation network. (b) Side view of the dislocated structure. (c) The strain field $(\varepsilon_{xx}+\varepsilon_{yy})/2$ calculated for Pt with the parameters $h=10$ ML and $s=32a_s$. The strain ranges from -0.9% (compressive) to 2.0% (tensile).

II. DENSITY FUNCTIONAL CALCULATIONS

A. Method

We use the first-principles quantum simulation method to accurately determine the energy barriers of surface diffusion processes. The quantum simulation method is based on DFT, and this method has been successfully applied to diverse surface systems.[6]

We employ the projector augmented-wave (PAW) method originally proposed by Blöchl.[7] We use its recent implementation by Kresse and Joubert.[8] The ultrasoft pseudopotential method is one of the most widely used methods for calculation of surface properties and, especially for $3d$ metals, improvement in the accuracy and savings in computation time can be significant. However, the pseudopotential for $3d$ metals is rather difficult to construct (particularly for magnetic elements), because too many parameters must be chosen (for example, several cutoff energies). Thus extensive testing is required in order to obtain an accurate pseudopotential. Many of these disadvantages are avoided in PAW.

The PAW method is a generalization of the well-known pseudopotential and linear augmented-plane-wave (LAPW) methods. It allows us to calculate with high accuracy electronic structure and related properties of solids and particularly *d* metals. The most important advantage is the possibility to calculate accurately the energy for magnetic systems of interest. PAW allows for relaxation of atomic configurations in a supercell, i.e., to find minimum energy. Knowledge of adatom relaxation on the surface is extremely important to accurately calculate energies of different adatom sites and barrier heights. We have performed test calculations for the Ag diffusion barrier on Pt(111) in the 7-layer slab geometry with 16 atoms in each layer of the periodic unit cell. We have used $3\times3\times1$ **k**-point sampling and the Monkhorst-Pack[9] integration scheme with smearing parameter $\sigma=0.2$ for relaxing the surface atoms. The final results were obtained using the Blöchl tetrahedron method with $5\times5\times1$ **k**-point sampling. The cutoff energy was 250 eV. We find the energy barrier to be 148 meV, in good agreement with experimental results[10] and previous calculations.[11] The same geometry is used for Co on Pt diffusion, except for the cutoff energy that was provided by the potentials for Co atoms to be 270 eV.

It is not easy to know all the important processes *a priori*. This may be demonstrated by an example of surface diffusion on fcc metal. Before Kellogg and Feibelman's report of concerted surface exchange,[12] the mechanism of simple adatom hopping was believed to be the lowest-energy barrier process for surface diffusion on fcc (001) surfaces. However, for the Al surface Feibelman demonstrated that simple adatom hopping is limited by a barrier of 0.65 eV. The energy barrier of the concerted surface exchange mechanism for this system is much lower, i.e., 0.20 eV (Ref. 13). According to this result, simple adatom hopping on Al(001) at room temperature is 36×10^6 times less likely to happen than concerted exchange.

For the Pt(111) surface the fundamental processes occurring during the early stages of epitaxial growth include adsorption from the vapor phase, surface diffusion of adatoms on the substrate, and the formation of stable and metastable islands.[14] There are two possible stacking sequences in the (111) direction of close-packed structures. The fcc structure has *ABCABC* stacking, while the hcp structure has *ABAB* stacking. An adatom on the surface can hop to two different stacking sites. Furthermore, the island grown on the surface may have two different edge types (depending on their geometry) with different Ehrlich-Schwoebel barrier. This may result in preferential growth of islands with only one edge type at low temperatures (triangular islands are grown), but with both edge types at higher temperatures (hexagonal islands).

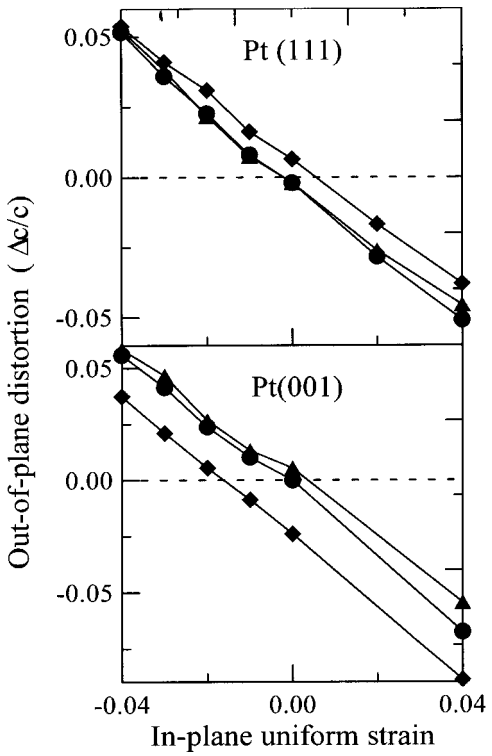

FIG. 2. Relaxation of the Pt layers with respect to the applied strain. Diamonds: induced strain between surface (first) layer and subsurface (second) layer. Circles: induced strain between second and third layer. Triangles: induced strain between third and fourth layers.

B. Pure Pt surface

Let us start from the density functional results for free Pt surfaces. The equilibrium bulk lattice constant *a* is calculated to be 3.91 Å, which corresponds to the experimental result of 3.92 Å. The seven-layer slab with periodic boundary conditions is constructed to simulate (111) and (001) surfaces of Pt. We optimize the distances *c* between Pt layers. We find that relaxation of the Pt surface layer is relatively small for the equilibrium lattice constant (see Fig. 2).

Then we perform the analysis of the effect of strain on the pure Pt(111) surface and compare the results with calculations for the Pt(001) surface. The uniform compressive strain is applied in the plane of the slab to find the elastic response of the system. The slab is allowed to relax in the perpendicular direction. This approach is usually referred to as the epi-

taxial Bain path (EBP). Uniform compressive strain in the plane of the slab causes increase in the distance between Pt layers both for (111) and (001) surfaces (as a solid tends to preserve the volume). Poisson's ratio obtained from these calculations for the (111) surface is 0.40. The experimental value for bulk Pt is 0.38. The in-plane stress for the seven-layer slab is 40 kbar (4 MPa) at equilibrium for the Pt(111) surface and 25 kbar (2.5 MPa) for Pt(001). The surface stress estimated by the slope of the EBP energy derivative at the bulk is equal to 5.5 N/m for the (111) surface and 4.3 N/m for the (001) surface.

C. Cobalt adsorption and diffusion on a Pt(111) surface

We consider adsorption of a Co atom on the Pt(111) surface as the first step in our study of Co film growth. We describe the dependence of the energy and magnetic moment on the Co atom as the function of the distance between the Pt surface and Co atom. The equilibrium distance for the adatom is equal to 1.79 Å, which is smaller than the interlayer distance of Pt films. Notice that a single Co atom introduces a large magnetic moment more than $3.6\mu_B$ (Bohr magneton)/per Co atom compared to the bulk moment of $1.6\mu_B$. The increase comes partly from increase of the Co spin moment to about $2\mu_B$, but it is mainly due to the polarization of Pt atoms around the adatom to about $0.14\mu_B$ for the first neighbors. This increase is similar to the single impurity effect in bulk systems where large moments for Fe and Co atoms were found due to the polarization of several shells of neighbors around the impurity atom. Thus it is important to know the magnetic state of the atoms on the surface for accurate energy description.

Let us define the ''cohesive'' energy of the adatom:

$$E_{\mathrm{coh}} = E^{\mathrm{slab}}_{\mathrm{Co\text{-}Pt}} - E^{\mathrm{slab}}_{\mathrm{Pt}} - E^{\mathrm{atoms}}_{\mathrm{Co}}, \tag{1}$$

where $E^{\mathrm{slab}}_{\mathrm{Co\text{-}Pt}}$ is the total energy of the slab with the Co adatom, $E^{\mathrm{slab}}_{\mathrm{Pt}}$ is the total energy of the slab without the Co adatom, and $E^{\mathrm{atoms}}_{\mathrm{Co}}$ is the energy of an isolated Co atom. Because the local density approximation (LDA) is not reliable for atomic energy calculations ($E^{\mathrm{atoms}}_{\mathrm{Co}}$), the results will have a systematic error. However, this error will be the same for all strains and it should not affect the results of growth modeling.

Figure 3 shows the variation of energy of an adatom as function of surface strain for three possible adatom locations on the free surface, i.e., fcc stacking site, hcp stacking site, and the bridge (or saddle) point between them. The latter is a saddle point for the hopping from one site to another. It is clear that the dependence is not simply linear. Moreover, the hcp location becomes more stable with increasing tensile strain and the curves cross at a tensile strain of approximately 0.02. This is quite different from Ag diffusion on the Pt(111) surface, where the energy dependence on strain is linear and the energy difference of hcp and fcc sites is strain independent. Figure 4 shows the potential energy barrier for hopping from fcc and hcp sites. It is clear that the barriers are almost linear functions of strain. They are crossing close to $\varepsilon = 0.02$. The hopping barrier for the unstrained system is approximately 0.3 eV.

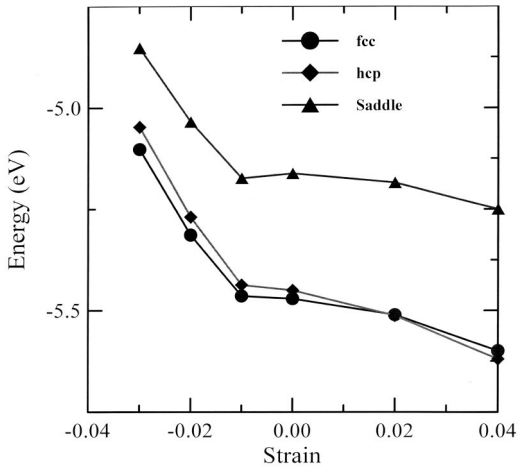

FIG. 3. Adatom energy of Co on the Pt(111) surface as a function of strain.

The magnetic moment per Co atom varies nonlinearly (see Fig. 5). It increases strongly for the compressive strain and does not change very much for tensile strain. This can be understood in terms of Pt polarization. At small strains the two first shells of neighbors feel the presence of the adatom and have significant polarization. For compressive strain the polarization of these atoms increases and includes additional neighbors. The magnetization variation correlates with the energy as a function of strain. For tensile strain there is little variation of the magnetic contribution to the energy and we see almost a linear strain dependence of the adatom energy, while for compressive strains we obtain a strong increase in the Pt magnetization. This results in a nonlinear energy variation.

The energy of the hcp site becomes lower than the fcc site at 2% tensile strain. It can be attributed to the energy connected with the magnetic polarization of Pt atoms as well. From the coordination point of view, the main difference between hcp and fcc sites is the presence of additional second-neighbor Pt atoms for the hcp site. For tensile strains

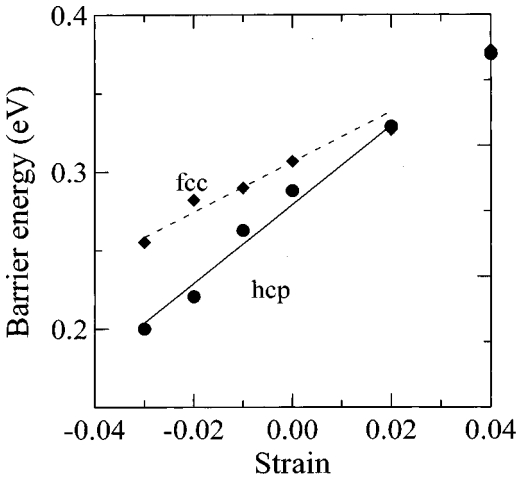

FIG. 4. Potential energy barriers for the hopping processes involving hcp and fcc sites. The dashed line represents the barrier dependence used in KMC simulations.

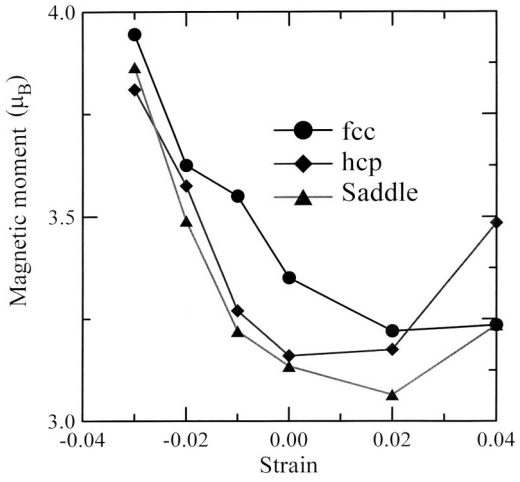

FIG. 5. Total magnetic moment per Co atom for the seven-layer slab geometry in fcc, hcp, and saddle sites.

this subsurface Pt atom in hcp stacking becomes polarized and interacts with the Co adatom, while this Pt atom is absent in fcc stacking. Thus, due to the magnetic energy of this pair, the energy of the hcp site is lowered relative to the fcc site. Ag on Pt(111) does not have this interaction, and the hcp site energy is always higher than that for the fcc site.

III. LINEAR ELASTIC THEORY OF SURFACE DIFFUSION

In order to understand the observed behavior let us consider the analysis of the problem using the linear elastic approximation (LEA). This is the traditional approach to determine the diffusion dependence of impurities on the external pressure.[16] Appendix A describes the relation of the activation volume approach in bulk systems to the surface diffusion problem.

By the definition of surface stress,[17]

$$\sigma_{ij}^{\mathrm{surf}}=\frac{1}{A}\frac{dE^{\mathrm{surf}}}{d\varepsilon_{ij}}=\tau_{ij}+\frac{1}{2}S_{ij\alpha\beta}\varepsilon_{\alpha\beta}, \tag{2}$$

where ε_{ij} is the surface-strain tensor and A is the equilibrium surface cell area, τ_{ij} is the intrinsic surface-stress tensor, and $S_{ij\alpha\beta}$ is the surface excess elastic modulus. In the LEA elastic constants are independent of strain (higher-order terms in the strains can be neglected) and the surface stress depends linearly on the strain.[17]

The effect of the adatom in this case can be described by the adatom-induced surface stress. It was shown by Wolf[18] that the surface stress is isotropic and diagonal at the surface of solids in its globally relaxed state (even for anisotropic surfaces). However, a surface is rarely found in a fully relaxed state. The strain dependence of stress may be quite strong.[18] In the case of nonmagnetic systems, the second term in Eq. (2) is quite insensitive to the presence of an adatom. The reason for this is that the adatom interacts with the free surface and is able to move out (in) with the applied compressive (tensile) strain. The change of the binding energy is very small, and the situation is similar to the case of a liquid where atoms are allowed to reconstruct. Thus the difference of the surface-stress tensor in the presence of an adatom on a pure surface is determined by the change in τ_{ij} due to the presence of the adatom. It means that the surface-stress tensor imposed by the adatom is almost independent of strain. This can be seen from several existing calculations.[19] If the surface is strained, the change in surface energy with adsorption due to the adatom can be written as

$$\Delta E=A\Delta\tau_{ij}\Delta\varepsilon_{ij}. \tag{3}$$

The diffusion tensor is determined by the barrier energy: i.e., the energy difference between stable valley ν (local energy has minimum) and saddle point s states. The change of the energy barrier is given then by

$$\Delta E=A(\sigma_{ij}^{\nu}-\sigma_{ij}^{s})\Delta\varepsilon_{ij}, \tag{4}$$

where σ_{ij}^{ν} and σ_{ij}^{s} are surface stresses induced by the adatom at the valley and saddle points, respectively.[20] These stresses can be evaluated numerically by either fitting energy data for different applied strains or directly calculating the stress tensor using the Hellman-Feynman theorem. The theory can be easily extended to surface defects such as steps (see Appendix B).

In the case of a magnetic adatom on a surface (like Co on Pt) the excess elastic modulus $S_{ij\alpha\beta}$ is sensitive to the presence of the adatom. Pt surface atoms become magnetically polarized when Co or other magnetic adatoms interact with them. This changes the elastic modulus, and the quadratic term becomes important. Note that the change in the adatom energy correlates well with the dependence of the slab magnetization on the applied strain. If the free energy is proportional to the magnetization squared, the energy variation is directly related to the polarization of Pt atoms near the adatom. However, for the barrier height no major deviations from the linear behavior were found. This is most probably related to the fact that $S_{ij\alpha\beta}$ depends similarly on the strain for both the ground state and saddle point.

This approach is good for small strains, i.e., when the linear elastic approximation is valid. When inelastic effects are important, the higher-order contribution should be included. Many calculations have been performed for surfaces of metals and semiconductors. All of them suggest, for small strain, that the linear elastic model works well for single-atom diffusion.

Transition metals and other free-electron-like materials are very similar in terms of their surface stress. The lack of coordination at the surface usually gives a tendency for surface bonds to contract. This results in an inward relaxation of the surface atoms. Thus for transition metals the surface stress is tensile, which is a consequence of the boundary conditions imposed on the wave functions in a Fermi gas model.[21] This does not take into account the redistribution of charges between *sp* and *d* orbitals. The slab calculations give smaller equilibrium lattice constants for planes perpendicular to the surface and support the above ideas.[22] For free-electron-like metals the bonds between adatoms and surface atoms are not directed and the system can lower its energy by relieving the surface stress without increasing its binding energy because of the change of the angle between adatom

and surface atom bonds. This means that $\Delta\tau_{ij}$ will be negative in Eq. (3). Thus the adatoms would tend to reside where the *tensile strain is maximized* because this would produce an overall lowering in energy. Equation (4) describes this also: i.e., there is a linear dependence on strain. Another argument can be made about the coordination of the adatom site. Adsorption sites with larger number of nearest neighbors will produce larger strain relief due to the fact that more surface bonds will be affected by the presence of an adatom. Because of this, the saddle point has smaller $\Delta\tau_{ij}$ than any of the valley (fcc or hcp) sites. Thus the energy barrier will grow with tensile strain as well. In terms of diffusion processes this means that atoms will have lower mobility at the sites of *largest tensile strain*. These are two major qualitative conclusions for free-electron-like metal surfaces.

Each adatom gives a contribution to the surface stress. Because of the interaction between adatoms and additional stresses associated with them, the induced stresses will depend on the coverage. After forming dimers and larger islands the additional misfit stress contribution to the total energy appears as well as stress associated with interactions between islands. Hence surface stress is expected to be a complicated function of surface coverage.

IV. KINETIC MONTE CARLO SIMULATIONS

The kinetic Monte Carlo model is a full-diffusion bond-counting model. It is a modified version of the model described in Ref. 5. In the present version of the model, the activation energy for diffusion E depends on the lattice mismatch $\Delta a/a_0$ at both the fcc sites and the saddle points, as well as the initial coordination number n_i and the final coordination number n_f. The following expression for E is used in the model:

$$E(\Delta a/a_0, n_i, n_f) = (n_i + n_f)E_{\text{saddle}}(\Delta a/a_0)/6 - n_i E_{\text{fcc}}(\Delta a/a_0)/3, \quad (5)$$

where $n_i E_{\text{fcc}}(\Delta a/a_0)/3$ is the binding energy on an fcc site and $E_{\text{fcc}}(\Delta a/a_0)/3$ represents the binding energy of one atomic bond. The term $(n_i+n_f)E_{\text{saddle}}(\Delta a/a_0)/6$ corresponds to the potential energy at the saddle point, where $E_{\text{saddle}}(\Delta a/a_0)/6$ is the saddle point energy corresponding to coordination number 1. (One discussion of this model with application to metals can be found in Ref. 29).

To incorporate the DFT results in the KMC model the energy strain dependences E_{fcc} and E_{saddle} for the fcc and saddle sites, respectively, plotted in Fig. 4 are approximated with linear relationships. This simplification might seem somewhat rough, however, comparing the strain dependence of the resulting potential energy barrier $E_{\text{fcc}}-E_{\text{saddle}}$ (bold line in Fig. 5) with the exact one (solid line in Fig. 5) demonstrates a very good correspondence that justifies the use of linear functions of the strain in the KMC simulations. The following expressions for E_{fcc} and E_{saddle} are used:

$$E_{\text{fcc}}(\Delta a/a_0) = E_{\text{fcc}}(0) + C_{\text{fcc}}\langle \Delta a/a_0 \rangle. \quad (6)$$

where $C_{\text{fcc}} = -3.75$ eV is the slope of the fcc site strain dependence, $E_{\text{fcc}}(0) = -4.0655$ eV is the unstrained binding energy for an adatom, and $\langle \Delta a/a_0 \rangle$ is the mean lattice mismatch averaged over the six nearest neighbors in the hexagonal surface cell. The second relationship is

$$E_{\text{saddle}}(\Delta a/a_0) = E_{\text{saddle}}(0) + C_{\text{saddle}}[\Delta a/a_0]_i, \quad (7)$$

where $C_{\text{saddle}} = -2.225$ eV is the slope of the saddle point strain dependence and $E_{\text{saddle}}(0) = -3.7624$ eV is the unstrained saddle point energy for an adatom hopping on a flat surface. The index i equals 1 or 2 and corresponds to the two-unit lattice vectors defining the hexagonal surface cell. Thus for the hexagonal surface the lattice mismatch is related to the strain in the following way:

$$[\Delta a/a_0]_1 = \varepsilon_{xx} \quad (8)$$

for the hexagonal unit vector $\mathbf{a}_1$ parallel to the x direction and

$$[\Delta a/a_0]_2 = (\varepsilon_{xx} + 3\varepsilon_{yy})/4 \quad (9)$$

for the hexagonal unit vector $\mathbf{a}_2$ oriented at the angle 60° relative $\mathbf{a}_1$.

Hence, for an arbitrary biaxial strain $(\varepsilon_{xx}, \varepsilon_{yy})$, the actual lattice mismatch can be calculated by using Eqs. (8) and (9) and the strain-modified fcc site and saddle point energies are easily calculated by applying Eqs. (6) and (7).

The strain field $(\varepsilon_{xx}, \varepsilon_{yy})$ for Pt on Pt(111) was calculated using Freund's continuum model.[15] It is assumed that a periodic hexagonal dislocation network with period $s = 32a_s$ (where a_s is the surface lattice constant) is confined to an interface buried below a capping layer of thickness $h = 10$ monolayers (ML). Figure 1 shows a schematic drawing of the structure under consideration and the resulting strain field $(\varepsilon_{xx} + \varepsilon_{yy})/2$, which is a good approximation for the biaxial strain at an fcc site. The strain ranges between -0.9% (compressive) and 2.0% (tensile).

In order to apply the strain dependence in the KMC model both $E_{\text{fcc}}(\Delta a/a_0)$ and $E_{\text{saddle}}(\Delta a/a_0)$ are discretized to 10 evenly spaced levels, which results in the possibility of 100 strain-related combinations on each lattice site. In addition, there is the possibility of equilibrium in the KMC, i.e., no strain. This gives totally 101 possible events for each (n_i, n_f) combination. Both n_i and n_f range independent of each other from 1 to 9, giving 81 coordination-related configurations. In the model there are also 8 step-edge diffusion related events, summing up to 89 basic events and totally including the strain we end up with 8989 events.

The hopping rate in the KMC model,

$$\nu(n_i, n_f, \varepsilon_{xx}, \varepsilon_{yy}) = \nu_0 \exp[-E(n_i, n_f, \varepsilon_{xx}, \varepsilon_{yy})/k_B T], \quad (10)$$

depends on both coordination numbers (n_i, n_f) and strains $(\varepsilon_{xx}, \varepsilon_{yy})$.[5,20] The attempt frequency ν_0 is conventionally chosen to $\nu_0 = 1 \times 10^{13}\ \text{s}^{-1}$. The simulations are performed on a lattice of size 256×128 sites.

The deposition rate and temperatures used in the simulations presented in Figs. 6 and 7 are 0.1 ML/s and -20 and 20 °C, respectively. All simulations are performed on fully strain-relaxed surfaces; i.e., the average surface strain is zero. Surface images from representative simulations are shown

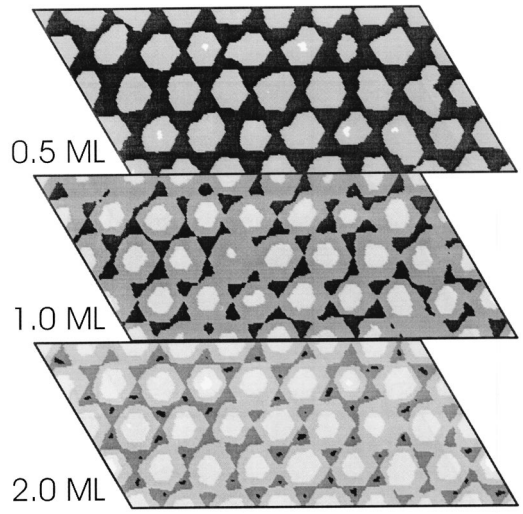

FIG. 6. Simulated surface images of Co growth on periodically strained Pt(111) at the temperature $T=-20\,^{\circ}\mathrm{C}$ showing the mechanism of strain-assisted self-organization.

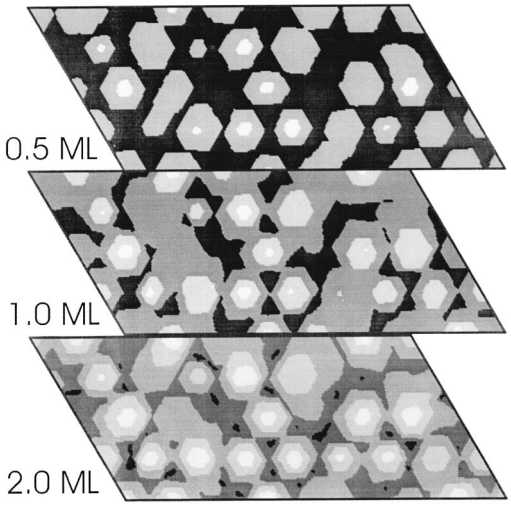

FIG. 7. Simulated surface images of Co growth on periodically strained Pt(111) at the temperature $T=20\,^{\circ}\mathrm{C}$. It is obvious that this temperature is too high to obtain well-characterized nanopatterning.

for three sequential coverages $\theta=0.5$, 1.0, and 2.0 ML, where white indicates the highest surface position and black represents the lowest one. It is obvious that the deposited adatoms have a tendency to nucleate at the intersections of the dislocations [Fig. 1(a)]. This is not surprising because these lattice sites have the highest tensile strain, indicating that the lattice parameter is largest there. This implies that it is easy for the lattice to accommodate the adatoms at these sites.

Experimentally, the growth was performed at room temperature, which resulted in well-shaped hexagonal islands for low coverage ($\sim$2 ML) and more triangular-shaped islands for higher coverage ($\sim$8 ML).[23] In the KMC simulations the step-edge diffusion is isotropic, so we expect the aspect ratio between adjacent (111) and (100) steps to be close to unity. Furthermore, only occupation of fcc sites is modeled. Tensile strains higher than 2% were not used in the simulations; the highest strain is just confined to the sharp strain-field maxima [cf. Fig. 1(a)]. Thus we are confident that the omission of hcp sites in the model does not significantly affect our results since our main interest in this study is strain-assisted self-organization and not whether the islands are fcc or hcp stacked.

Representative KMC results for the temperature $T=-20\,^{\circ}\mathrm{C}$ on the one hand gives periodically self-organized fairly hexagonal-shaped islands, as shown in Fig. 6. On the other hand, for $T=20\,^{\circ}\mathrm{C}$ it is evident that the temperature is too high for well-characterized self-organization to take place: however, parts of the surface are still periodically self-organized (cf. Fig. 7). Another observation is that second-layer (and also higher-layer) islands grow faster at $T=20\,^{\circ}\mathrm{C}$ than for $T=-20\,^{\circ}\mathrm{C}$. This is obvious when the surface images generated at 0.5 ML coverage in Figs. 6 and 7 are compared. The observation can be explained by the fact that the electron spin (ES) barrier is more effective for straight step edges than for rough ones.

In terms of the application of cluster systems for magnetic recording, small and flat islands cannot be used in devices because their volume V is extremely small. The reason for this is that their anisotropy barrier KV is small (K is the anisotropy constant per unit volume), so that they are superparamagnetic down to very low temperatures. Describing superparamagnetism, let us consider a single cluster. In zero applied field, a cluster with high uniaxial anisotropy K can be in two states, either up or down. At temperature $T=0$ K, the magnetization is frozen: i.e., the dot is fully remanent. When thermal energy becomes too large, i.e., about $25k_BT/KV$ (k_B is Boltzmann's constant), the dot is superparamagnetic. This means that the spin fluctuates between up and down, even though the particle remains ferromagnetic: i.e., all electronic spins within a cluster remain aligned with each other at any given time. The crossover between the two regimes occurs at the blocking temperature T_B, determined experimentally by the cancellation of remanent magnetization. The small value of V cannot be compensated by a high value of K, because anisotropy fields of the order of several tens of teslas would be required to obtain $T_B=300$ K. The possible solution is to increase V by using vertical pillars instead of flat dots. Vertical pillars could be fabricated by repeating the deposition of Pt and Co layer by layer.[3] In this case one can obtain both pillars of Co or Co/Pt multilayers.

V. CONCLUSIONS

We performed an analysis of the surface diffusion and growth of Co on strained Pt(111) surfaces. We show that the Co adatom energy decreases with tensile strain, while the barrier height for the hopping process increases with tensile strain. The diffusion is affected by the polarization of Pt surface sites, resulting in nonlinear behavior of the cohesive energy as a function of strain. The barrier height for diffusion processes depends linearly on strain. We analyzed the DFT results using linear elastic theory. We demonstrated that the KMC method can be used to perform realistic simulations of strain-assisted self-organization of nanostructures by includ-

ing strain-related results from both continuum calculations and atomistic first-principles DFT calculations. We have also presented simulations of Co nanopatterning on periodically strained Pt(111) surfaces. The simulations indicate that the nucleation is strongly favored on lattice sites with high tensile strain; however, selecting the optimal growth temperature is crucial since the self-organization can easily be destroyed at high temperatures.

ACKNOWLEDGMENTS

This work is supported by NSF Grant No. EEC-0085569. Density functional calculations were performed on the National Energy Research Scientific Computing Division (NERSC) facility and supported by Computational Materials Science Network. Kinetic Monte Carlo simulations were performed at the Sun cluster at the Department of Physics, Karlstad University, Sweden.

APPENDIX A: LINEAR ELASTIC THEORY OF ADATOM BULK DIFFUSION AND ITS CONNECTION TO SURFACE DIFFUSION

The diffusion of adatoms in the bulk is usually analyzed in terms of an activation volume that can be obtained from the experimental dependence of diffusivity on pressure and temperature:

$$V^* = -k_B T \frac{\partial \ln D(T,p)}{\partial p}, \tag{A1}$$

where p is pressure, D is diffusivity, T is temperature, and k_B is Boltzmann's constant. This volume is change in the volume associated with formation of defect in the ground state and at the saddle point. The work needed to account for this volume change is equal to pV^*. This makes the definition of the activation volume natural and the energy associated with the applied stress is $E = V^* \sigma$, where σ is the applied stress (pressure, in the hydrostatic case). We refer reader to Ref. 24 for more details on the elasticity theory for bulk diffusion. Even for nonhydrostatic pressure the stress-strain work required approach can be generalized.[25] Assuming that the activation volume does not depend strongly on stress, it is a useful parametrization. If the applied strain is known, the energy can be rewritten using the proportionality of strain and stress ($\sigma = Y\varepsilon$, where Y is the elastic modulus). The similarity with the surface diffusion is obvious.

Analysis of diffusion at the surface, presented in this paper, is somewhat different and uses language of ''induced stress strain.'' [20] The reason for this is convenience. For the bulk system when the stress (pressure) is known the activation volume tensor is more convenient to use, while for the surface the strain is known. It is possible to apply the activation volume approach to the surface. The area tensor associated with the adatom should be defined. There are some difficulties, at first glance, in using the activation volume analysis for the surface. First of all, the surface has its own surface stress at the ground state. The adatom is usually not located in the plane of the surface and is free to move: i.e., it does not have a well-defined volume. The relaxation of surface atoms on metal surfaces is usually mostly perpendicular to the surface plane (mostly inward). There is not much area change when an adatom is present. Thus the surface with an adatom is not exactly a two-dimensional object. In this sense the description of the problem through the forces induced by the adatom is more physically transparent. The formulation can be done in an ''activation-volume–stress'' formalism as well, but the activation area has a complicated connection with the actual displacements of the atoms in the surface layer.

The problem with the volume tensor definition is its locality. Activation volume, associated with the impurity, is not sensitive to the position of other impurities and defects such as interface, surface, etc. However, a nonlocal volume tensor can be introduced. It is possible to rewrite the theory in a more transparent way. Besides the ''volume-tensor–stress'' formulation, it is possible to consider the problem through the stress induced by the impurity. In this formulation, instead of considering displacements of atoms due to the presence of an impurity, the forces that are needed to perform these displacements are considered. The elastic energy change associated with the applied strain can be rewritten as follows:

$$\Delta E = V\sigma^*\varepsilon + O(\varepsilon^2), \tag{A2}$$

where σ^* is the excess stress induced by the impurity on the lattice. In this form bulk and surface considerations are similar and a clear connection can be seen. Still, if an experiment with known pressure is performed, the activation volume idea is easier to use.

The formulation, presented in this appendix, is valid only if linear elastic theory is applied and there are no additional contributions. In the case of magnetic impurities the activation volume (or impurity-induced strain) may be sensitive to the strain because magnetic moments can be induced around the impurities and the strength of the magnetic interaction will change with the strain.

APPENDIX B: LINEAR ELASTIC THEORY OF ADATOM DIFFUSION OVER THE ERLICH-SCHWOEBEL BARRIER

Wolf[18] has shown that the surface stress is isotropic and diagonal at the surface of solids in its globally relaxed state (even for anisotropic surfaces). In this appendix we show that the presence of extended defects should in principle break this conclusion. We use the step edge (or island edge) as an example.

The energy of the surface with the step edge can be expanded in a Taylor series with terms related to the intrinsic tensor and the excess elastic modulus. Because atoms at the step edge will have missing bonds compared to the surface atoms, the interactions between atoms in the edge will be different. This contribution of such ''excess'' interactions to the surface energy can be called edge energy in analogy with surface energy. Note that this is the energy due to different strength of the interaction at the edge and not a simple discontinuity of surface stress that can be treated by integration with the static Green's tensor of elasticity theory.[26]

Because the edge is a linear defect (can be viewed as a linear chain), we expect that energy will be sensitive mainly to the elastic strain along the edge direction. Then, keeping only strain vectors in the expansion in the Taylor series, the linear edge stress is given by

$$\sigma_i^{\text{edge}} = \tau_i + \frac{1}{2} S_{ij} \varepsilon_j , \tag{B1}$$

where τ_i is the *intrinsic* elastic force of the edge at equilibrium and S_{ij} is the excess modulus associated with the edge. Note that steps give ''anisotropic'' (i.e., directed) contributions to the elastic forces on the surface. When the second term is not sensitive to the presence of the adatom (most nonmagnetic systems), we find again that the energy of the adatom has a linear dependence on the strain. The total effect on the adatom energy at valley and saddle sites includes both surface-stress tensor and edge-stress vector differences. The edge stress contribution to the energy of the system is

$$\Delta E = A(\sigma_i^{\text{edge},v} - \sigma_i^{\text{edge},s}) \varepsilon_i . \tag{B2}$$

For adatom hops across the step edge, for example, the total energy of the adatom consists of both surface and edge contributions at the valley site, while at the saddle point only edge effects contribute. The total intrinsic surface stress of a surface with a step edge includes surface and edge contributions. The barrier energy for over-the-edge hop is a linear function of strain, similar to the hopping diffusion on the ideal surface.

The consideration of the elastic field due to the step in the direction perpendicular to the step is given by Marchenko and Parshin.[27] Adatoms interact with the step due to the elastic strain field of the step.[27,28] This will effectively change the intrinsic surface-stress tensor as a function of distance from the step. This should be taken into account when modeling diffusion.

The LEA used in the above analysis does not include changes in the electronic structure with strain and other inelastic terms. For example, if an ideal square surface is strained in the *x* direction, it should not affect the motion in the *y* direction. This is generally not true, and it has been shown previously.[29] The effect can be assumed small. However, nonlinear terms can be included in the consideration.

*On leave from Department of Physics, Karlstad University, Sweden.

[1] H. Neal Bertram, *Theory of Magnetic Recording* (Cambridge University Press, Cambridge, England, 2001).
[2] S. Landis, B. Rodmacq, and B. Dieny, Phys. Rev. B **62**, 12 271 (2000).
[3] O. Fruchart, M. Klaua, J. Bartel, and J. Kirschner, Phys. Rev. Lett. **83**, 2769 (1999).
[4] K. Bromann *et al.*, Eur. Phys. J. D **9**, 2528 (1999).
[5] M. I. Larsson, Phys. Rev. B **64**, 115428-1 (2001).
[6] G. Kresse and J. Furthmüller, Comput. Mater. Sci. **6**, 15 (1996).
[7] P. Blöchl, Phys. Rev. B **50**, 17 953 (1994).
[8] G. Kresse and D. Joubert, Phys. Rev. B **59**, 1758 (1999).
[9] H. J. Monkhorst and J. D. Pack, Phys. Rev. B **13**, 5188 (1976).
[10] H. Brune, K. Bromann, H. Röder, K. Kern, J. Jacobsen, P. Stoltze, K. Jacobsen, and J. Nørskov, Phys. Rev. B **52**, R14 380 (1995).
[11] C. Ratsch, A. P. Seitonen, and M. Scheffler, Phys. Rev. B **55**, 6750 (1997).
[12] G. L. Kellogg and P. J. Feibelman, Phys. Rev. Lett. **64**, 3143 (1990).
[13] P. J. Feibelman, Phys. Rev. Lett. **65**, 729 (1990).
[14] P. J. Feibelman, Phys. Rev. B **60**, 4972 (1999); S.-L. Chang and P. A. Thiel, Crit. Rev. Surf. Chem. **3(3/4)**, 239 (1994).
[15] L. B. Freund, Adv. Appl. Mech. **30**, 1 (1994).
[16] R. N. Jeffrey and D. Lasarus, J. Appl. Phys. **41**, 3186 (1970).
[17] R. Shuttleworth, Proc. Phys. Soc. London, Sect. A **63**, 444 (1950).
[18] D. Wolf, Phys. Rev. Lett. **70**, 627 (1993).
[19] The linearity of the energy barrier on the strain was shown in E. Penev, P. Kratzer, and M. Scheffler, Phys. Rev. B **64**, 085401 (2000); C. Ratsch, A. P. Seitonen, and M. Scheffler, *ibid.* **55**, 6750 (1997); Schindler and D. E. Wolf, in *Structure and Dynamics of Heterogeneous Systems*, edited by P. Entel and D. E. Wolf (World Scientific, Singapore, 2000). D. Crzan (private communication).
[20] H. T. Dobbs, A. Zangwill, and D. D. Vvedensky, in *Surface Diffusion: Atomistic and Collective Processes*, edited by M. Tringides (Plenum, New York, 1997), p. 263.
[21] See, for example, F. Garcia-Moliner and F. Flores, *Introduction to the Theory of Solid Surfaces* (Cambridge University Press, Cambridge, England, 1979), p. 146.
[22] P. M. Marcus, X. Qian, and W. Hubner, J. Phys.: Condens. Matter **12**, 5541 (2000).
[23] Lundgren, B. Stanka, M. Schmid, and P. Varga, Phys. Rev. B **62**, 2843 (2000).
[24] P. H. Dederichs and K. Shroeder, Phys. Rev. B **17**, 2524 (1978).
[25] Y. Zhao, M. Aziz, H.-J. Gossmann, S. Mitha, and D. Schiferl, Appl. Phys. Lett. **74**, 31 (1999).
[26] V. Shchukin and D. Bimberg, Rev. Mod. Phys. **71**, 1125 (1999).
[27] V. I. Marchenko and A. Ya. Parshin, Zh. Eksp. Teor. Fiz. **79**, 257 (1980) [Sov. Phys. JETP **52**, 129 (1980)]. See also L. E. Shilkrot, and D. J. Srolovitz, Phys. Rev. B **53**, 11 120 (1996).
[28] L. E. Shilkrot and D. J. Srolovitz, Phys. Rev. B **55**, 4737 (1997).
[29] J. Merikoski, I. Vattulainen, J. Heinonen, and T. Ala-Nissila, Surf. Sci. **387**, 167 (1997).